Particle electrification and levitation in a continuous particle feed and dispersion system with vibration and external electric fields

AUTHOR(S):

Shoyama, Mizuki; Kawata, Takumu; Yasuda, Masatoshi; Matsusaka, Shuji

CITATION:

Shoyama, Mizuki ...[et al]. Particle electrification and levitation in a continuous particle feed and dispersion system with vibration and external electric fields. Advanced Powder Technology 2018, 29(9): 1960-1967

ISSUE DATE:

2018-09

URL:

http://hdl.handle.net/2433/234593

Advanced Powder Technology 29 (2018) 1960–1967

Contents lists available at ScienceDirect

Advanced Powder Technology

journal homepage: www.elsevier.com/locate/apt

Original Research Paper

Particle electrification and levitation in a continuous particle feed and dispersion system with vibration and external electric fields

Mizuki Shoyama, Takumu Kawata, Masatoshi Yasuda, Shuji Matsusaka *

Department of Chemical Engineering, Kyoto University, Kyoto 615-8510, Japan

ARTICLE INFO

Article history:
Received 31 December 2017
Received in revised form 16 April 2018
Accepted 21 April 2018
Available online 6 June 2018

Keywords:
Particle electrification
Levitation
Dispersion
Electric field
Vibration

ABSTRACT

Electrification and levitation of particles in a continuous particle feed and dispersion system have been studied both theoretically and experimentally. This system consisted of a vibrator and inclined parallel electrodes. A mesh and a vibrating plate were used for the upper and lower electrodes, respectively. A dc voltage was applied to one of the electrodes and the other electrode was grounded. Particles fed to the lower electrode were charged by induction and levitated upward by the Coulomb forces. When the applied voltage was high enough, the particles passed through the mesh electrode. The charge of the particles was measured with a Faraday cup, and the particle behavior was observed with a high-speed microscope camera. The particle charges were also analyzed from experimentally obtained particle trajectories and numerically calculated electric fields. Finally, the conditions for the effective levitation and dispersion of the charged particles and their mechanisms were studied and have been described in detail.

1. Introduction

In powder handling processes, continuous feeding is essential for stable operation and the quality control of products. However, small particles tend to agglomerate together and adhere to surfaces. These phenomena may cause the loss of operability and productivity [1]. To disperse the agglomerated particles, airflows have been widely used [2,3]. Vibration is also effective to prevent the particles from adhering to the surfaces without the use of airflows [4,5]. Furthermore, electrostatic repulsion forces between particles with a unipolar charge can be used for dispersion [6]. By using the forces caused by static electricity and vibration, the reliability of continuous particle feeding and dispersion will be improved.

Parallel plate electrodes create a uniform electric field, and the motion of particles between the electrodes is controlled by the electric field strength and direction. When conductive particles contact one of the electrodes, they are charged by induction. The polarity of the particles is the same as that of the electrode. When Coulomb forces acting on the charged particles overcome the oppositely directed forces, such as adhesion and gravity, the particles are levitated from the electrode. High-conductivity particles are instantaneously charged by induction [7]. However, if the conductivity of the particles is low, a longer time is required for them to charge [8–11]. Furthermore, if the resistance of the material is extremely high, the particles cannot be charged by the induction but rather by contact charging based on the contact potential difference between the particles and the electrode [12,13]. Because the quantity of charge transferred during a single contact is generally small, the particles cannot levitate from the electrode. On the other hand, in the case of induction charging, as the quantity of transferred charge is rather large, the particles can levitate and move toward the counter electrode. When the particles contact the counter electrode, the polarity of the particles inverts because of induction charging. After changing the charge (sign and value) the particles will move in the opposite direction. As a result, the particles oscillate between the parallel electrodes [7]. Therefore, there are positively and negatively charged particles between the electrodes even if a dc voltage is applied.

To extract particles with a unipolar charge, openings may be needed in one of the parallel electrodes [14]. Replacing the upper plate electrode with a mesh electrode allows the passage of the particles through the openings. When the particles above the upper electrode all have the same charge polarity, they can be dispersed by their mutual electrostatic repulsion.

Motion of particles can also be controlled by using ac electric fields. When multi-phase ac voltages are applied to the comb-type electrodes, the particles close to the electrodes experience repulsion from the electrodes [15]. For example, there are applications related to the control of particle position [16], classification

* Corresponding author.
E-mail address: matsu@cheme.kyoto-u.ac.jp (S. Matsusaka).

https://doi.org/10.1016/j.apt.2018.04.022

Nomenclature

C_d	drag coefficient (–)
D_p	particle diameter (m)
E_{ex}	external electric field strength in the z-direction (V/m)
F_d	drag force (N)
F_e	electrostatic force (N)
F_{ex}	Coulomb force in the external electric field (N)
F_g	gravitational force (N)
F_{grad}	gradient force (N)
F_i	image force (N)
$F(z_p)$	cumulative distribution of particle positions in the z-direction (–)
$F(z_{pmax})$	cumulative distribution of highest particle positions in the z-direction (–)
g	gravitational acceleration (m/s^2)
m_p	mass of primary particle (kg)
q_m	specific charge (charge-to-mass ratio) (C/kg)
q_p	charge of primary particle (C)
q_{pe}	equilibrium charge of primary particle (C)
Re_p	particle Reynolds number
t	time (s)
v_p	particle velocity (m/s)
x	longitudinal coordinate (m)
y	transverse coordinate (m)
z	height coordinate (m)
z_p	particle position in the z-direction (m)
z_{pmax}	highest particle position in the z-direction (m)
ε_0	vacuum permittivity = 8.85 × 10^{-12} (F/m)
ε_r	relative permittivity of fluid (–)
ε_{rp}	particle relative permittivity (–)
θ	inclination angle of plate (°)
μ	viscosity of fluid (Pa·s)
ρ	density of fluid (kg/m^3)
ρ_p	particle density (kg/m^3)
ρ_v	particle volume resistivity (Ω·m)
τ	relaxation time (s)

[17], separation [18], and surface cleaning [19,20]. Furthermore, there are many reports regarding particle levitation using various forms and configurations of electrodes [21,22]. The electric fields allow particles to charge and move even in the absence of complicated mechanical and/or pneumatic systems. Thus, electrostatic techniques are expected to be useful for complex applications like space exploration [20,22] as well as operation under atmospheric pressure.

In powder handling processes, a conceptual system using parallel electrodes with vibration has been proposed for continuous particle feeding and dispersion [23,24]. This system can also be used for the electrostatic characterization of particles [25], where the particles are not charged by induction charging but by contact charging based on the contact potential difference.

Particle charging in a strong electric field system with a mesh electrode should be useful for continuous particle feeding and dispersion. However, the particle charge and levitation depend on conditions such as the electric field strength and direction, adhesion and gravity, among others [26]. Thus, the effect of these factors should be clarified to develop a continuous particle feed and dispersion system.

The goal of this research was to develop a new system for continuous particle feeding and dispersion using a vibrator and inclined parallel electrodes. A mesh electrode and a vibrating plate electrode were used for the upper and lower electrodes, respectively. The charge of the particles was measured under various conditions and the particle behavior was observed microscopically. Furthermore, the particle charges were analyzed from experimentally obtained particle trajectories and numerically calculated electric fields; moreover, the levitation and dispersion of the charged particles were studied, and have been discussed in detail.

2. Experimental setup and procedure

Fig. 1 shows a schematic diagram of the experimental setup, which consists of a particle feeder and a disperser using a vibrator and parallel electrodes. A stainless steel plate (SUS 304, 35 × 50 mm) that was attached to an acrylic base inclined at an angle of 15° from horizontal was used for the lower electrode. A stainless steel mesh (SUS304, 35 × 50 mm, wire diameter: 0.6 mm, opening: 3.63 mm) was used for the upper electrode, which was placed at a distance of 20 mm from the lower electrode. One of the electrodes

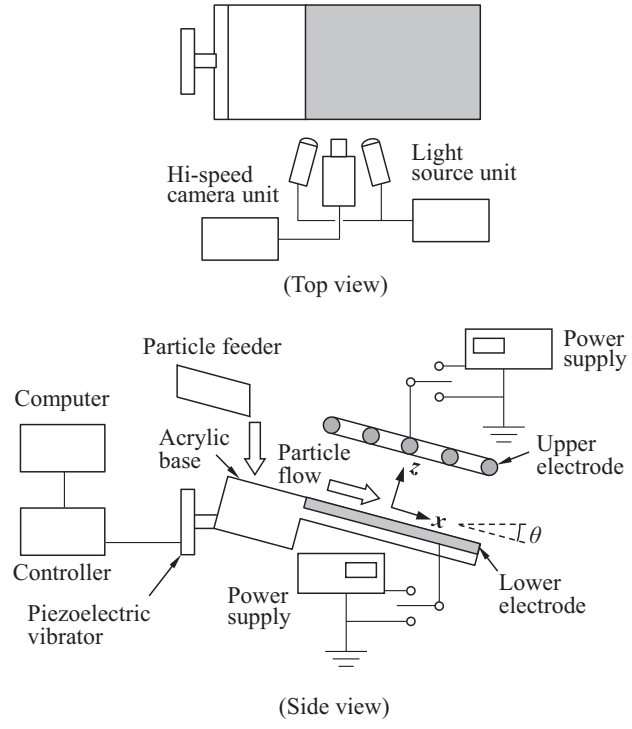

Fig. 1. Experimental setup.

was connected to a power supply (610D, Trek Inc.), and a dc voltage ranging from −8 to +8 kV was applied, while the other electrode was grounded. Particles were fed at a constant mass flow rate (20 mg/s) and transported on the lower electrode, which was vibrated by a piezoelectric vibrator to assist the flow of the particles. The amplitude and frequency of the vibration of the plate electrode were set at 20 μm and 300 Hz, respectively, by a controller (VST-01, IMP Co., Ltd.) To measure the specific charge, i.e., the charge-to-mass ratio of the particles, a Faraday cup and an electrometer (8252, ADC Corporation) was used. In addition, the behavior of the particles in this system was observed through a high-speed camera (FASTCAM Mini UX100, Photron Ltd.) with a high-magnification zoom lens (VSZ-10100, VS Technology Corpo-

ration) at a frame rate of 4000 fps. Two metal halide lamps (LS-M250, Sumita Optical Glass, Inc.) were used as the light source.

Alumina particles with a mass median diameter of 48 μm and a geometric standard deviation of 1.2 (Showa Denko K.K.) were used. The Sauter diameter was 47 μm. The particle density (ρ_p) and the particle relative permittivity (ε_{rp}) were 3800 kg/m^3 and 9, respectively. The particle volume resistivity (ρ_v) was 0.1 GΩ m, which was measured at a low consolidation pressure (0.15 MPa). The particles were dried at 120 °C for 12 h and cooled to room temperature in a desiccator before use. All the experiments were carried out under room conditions, i.e., temperature: 25 ± 5 °C and relative humidity: 45 ± 5%.

3. Numerical calculation of electric fields

External electric fields in this system were calculated by a finite element method (COMSOL Multiphysics, AB/COMSOL, Inc.) assuming a three-dimensional model in a Cartesian coordinate system. The distance between the upper and lower electrodes and the configuration of the mesh electrode were the same as those in the experimental setup. The electric potentials at the edges of the domain (x = ±175 mm, y = ±250 mm, z = ±100 mm) were assumed to be zero. The center of the mesh electrode, (x, y) = (0, 0), is also the center of the wire mesh opening.

Fig. 2 shows numerically calculated electric potential distributions. The upper electrode voltage (V_U) and the lower electrode voltage (V_L) were given. The potential difference between the two electrodes ($\Delta V_{L-U} = V_L - V_U$) was set at +8 kV. For V_L = +8 kV and V_U = 0 (Fig. 2a), the interval of equipotential lines, or potential gradient, between the electrodes was almost constant except around the upper electrode. The calculated result for V_L = 0 and V_U = −8 kV (Fig. 2b) was similar to that in Fig. 2a; however, the potential gradient above the upper electrode was larger. This difference is caused by the potential difference between the upper electrode and the top of the domain.

Fig. 3a shows the profiles of electric field strength (E_{ex}) along the z-axis at x = 2.12 and y = 0. The mesh electrode with 0.6 mm wire diameter was located from z = 20 to 20.6 mm. A uniform electric field was formed between the upper and lower electrodes; however, the electric field changed drastically around the mesh electrode because of electric field lines concentration at the mesh wires. The electric field was directed upward below the upper electrode, and downward above the upper electrode. Similar calculated results were also obtained in the previous study [26]. Above the upper electrode, $E_{ex} \approx 0$ for V_U = 0, and $E_{ex} < 0$ for V_U = −8 kV.

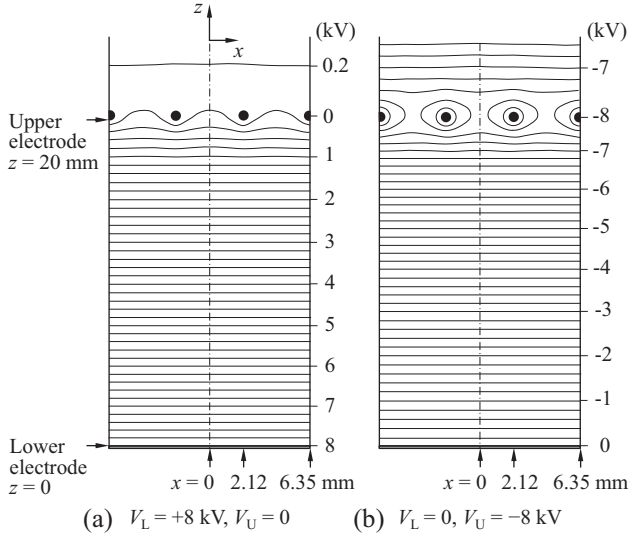

Fig. 2. Electric potential distributions calculated by the finite element method.

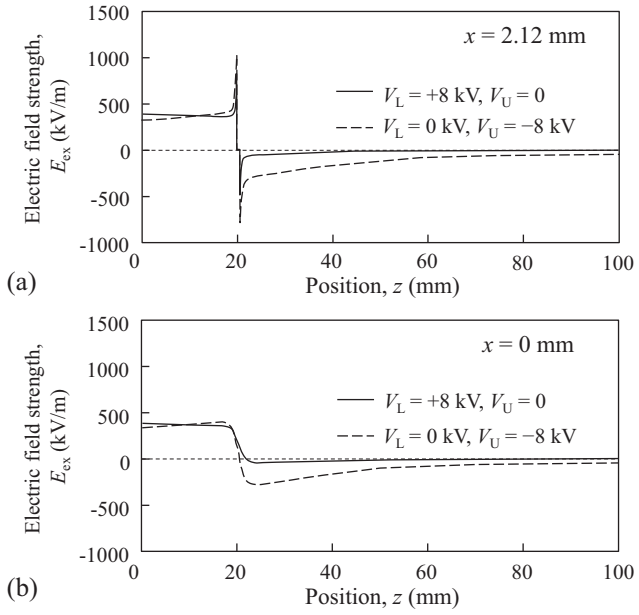

Fig. 3. Profiles of electric field strength along the z-axis: (a) x = 2.12 and y = 0 (the center of a wire of the mesh electrode); and (b) x = 0 and y = 0 (the center of the wire mesh opening).

Fig. 3b shows the electric field strength profile at x = 0 mm and y = 0, which corresponds to the center of the wire mesh opening. E_{ex} was almost constant between the upper and lower electrodes, but decreased around the upper electrode. In the case of z > 25 mm, the E_{ex} values were almost the same as those in Fig. 3a.

The charged particles in the electric fields experience Coulomb forces depending on the electric field strength and direction. Hence, the difference in the electric fields at z > 25 mm, which is related to the applied voltage on the upper electrode, affects the behavior of the particles above the upper electrode.

Fig. 4a shows the effect of voltage applied to the lower electrode on the profile of the electric field strength at x = 2.12 and y = 0, when V_U = 0. As a matter of course, the E_{ex} value depends on V_L at z < 25 mm. On the other hand, Fig. 4b shows that V_U affects E_{ex} even at z > 25 mm. These calculated profiles of the electric field strength can be used for particle motion analysis.

4. Estimation of particle charge based on motion analysis in an electric field

A particle in an electric field experiences an electrostatic force (F_e), a gravitational force (F_g), and a drag force (F_d). The equation of motion of a particle in the z-direction is given by

$$m_p \frac{dv_p}{dt} = -F_d - F_g + F_e, \quad (1)$$

where m_p is the mass of the particle, vp is the particle velocity, and t is the time. The mass of the particle is given by

$$m_p = \frac{\pi {D_p}^3 \rho_p}{6}, \quad (2)$$

where D_p is the particle diameter and ρ_p is the particle density. For a stationary fluid, F_d is given by

$$F_d = C_d \frac{\pi {D_p}^2}{4} \frac{\rho_p {v_p}^2}{2}, \quad (3)$$

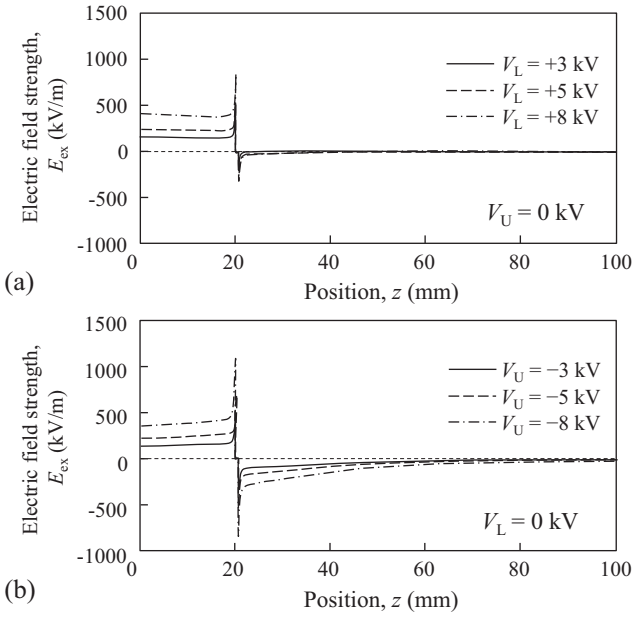

Fig. 4. Effect of voltage applied to an electrode on electric field strength at $x = 2.12$ and $y = 0$: (a) $V_U = 0$ and $V_L > 0$; and (b) $V_L = 0$ and $V_U < 0$.

where C_d is the drag coefficient, which is given by [27].

$$C_d = \frac{24}{Re_p}\left(1 + 0.15Re_p^{0.687}\right) \text{ for } Re_p \leqslant 1000 \tag{4}$$

and

$$Re_p = \frac{\rho v_p D_p}{\mu}, \tag{5}$$

where ρ and μ are the density and the viscosity of the fluid, respectively. The gravitational force on the particle in the z-direction is given by

$$F_g = m_p g \cos\theta, \tag{6}$$

where g is the gravitational acceleration and θ is the inclination angle of the plate electrode from the horizontal. F_e consists of the Coulomb force in the external electric field (F_{ex}), the image force (F_i) and gradient force (F_{grad}):

$$F_e = F_{ex} - F_i - F_{grad}. \tag{7}$$

When the particle levitates from the electrode, F_i and F_{grad} act in the reverse direction to F_{ex}, which is given by

$$F_{ex} = q_p E_{ex}, \tag{8}$$

where q_p is the particle charge and E_{ex} is the external electric field strength. Here, F_i is given by

$$F_i = \frac{q_p^2}{16\pi\varepsilon_r\varepsilon_0 z_p^2} \tag{9}$$

where ε_r is the relative permittivity of the fluid, ε_0 is the vacuum permittivity, and z_p is the distance of the particle from the surface of the electrode. F_{grad} is given by [28]

$$F_{grad} = \frac{\pi\varepsilon_0\varepsilon_r(\varepsilon_p - 1)}{4(\varepsilon_p + 2)} D_p^3 \text{grad} E_{ex}^2 \tag{10}$$

Using the above equations, the position of the charged particle as a function of elapsed time was sequentially calculated. From the comparison of the experimentally obtained trajectory with numerically calculated one, the particle charge can be determined [26].

Space charge caused by charged particles can affect the particle motion; however, particle volume concentration in this study is 0.004% at $z = 0$–40 mm and the space charge effect is estimated to be 10% or less. For simplicity, we exclude this factor from the analysis.

5. Analysis of induction charging

The equilibrium charge of a conductive particle by induction charging is represented by [7]

$$q_{pe} = 1.65\pi\varepsilon_r\varepsilon_0 D_p^2 E_{ex}. \tag{11}$$

The equilibrium charge of a dielectric particle is represented by [10]

$$q_{pe} = 0.55p\pi\varepsilon_r\varepsilon_0 D_p^2 E_{ex}, \tag{12}$$

where p is given by

$$p = \frac{3\varepsilon_{rp}}{\varepsilon_{rp} + 2}, \tag{13}$$

where ε_{rp} is the particle relative permittivity.

The particle charge as a function of time is expressed as

$$q_p(t) = q_{pe}[1 - exp(-t/\tau)], \tag{14}$$

where τ is the relaxation time, which is given by

$$\tau = \rho_v\varepsilon_0\varepsilon_{rp} \tag{15}$$

where ρ_v is the particle volume resistivity.

6. Results and discussion

6.1. Particle behavior and levitation height

Fig. 5 shows a photograph of the particles moving on the lower electrode that is vibrating. Here, the upper and lower electrodes were grounded ($V_U = V_L = 0$). Since there was no external electric field, particle levitation caused by Coulomb forces did not occur. The particles were simply transported on the inclined electrode, and finally fell at the edge of the electrode. When the vibration was stopped, the stable particle flow was not maintained; therefore, the vibration and gravity both contribute to the particle flow.

Fig. 6 shows the photographs of particle behavior under different conditions, where an external voltage was applied to one of the electrodes. The particles were spread in three-dimensional space. This can be explained as follows; when the particles contact the lower electrode, charge transfers occur, and the particles experience Coulomb forces. When these forces are large enough, the par-

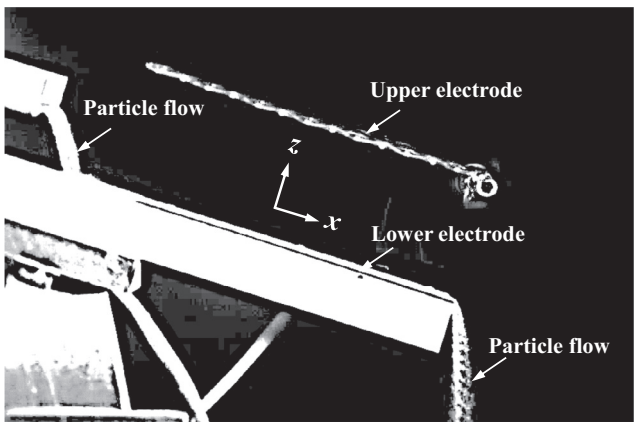

Fig. 5. Particle behavior on the vibrating electrode ($V_U = V_L = 0$).

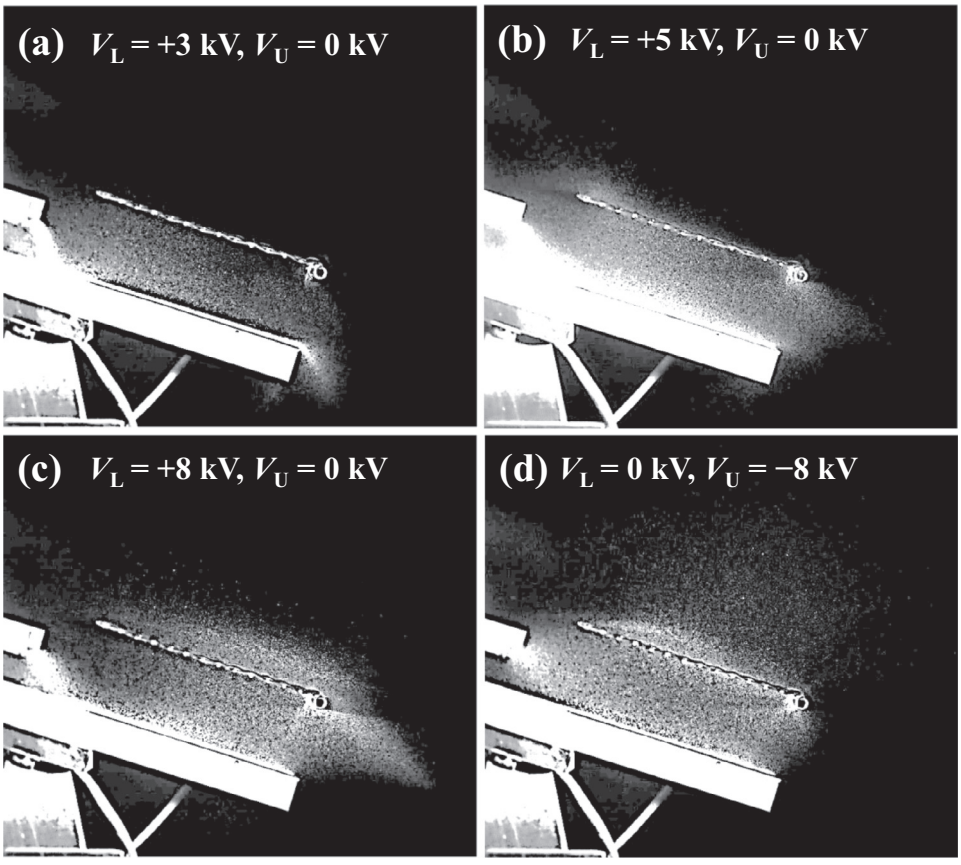

Fig. 6. Variation of particle behavior under different applied voltages.

ticles are levitated. However, even if the Coulomb forces of the levitated particles are not very large, the particles fall eventually because of gravity. For V_L = +3 kV and V_U = 0 (Fig. 6a), the particles on the lower electrode were levitated and spread between the upper and lower electrodes. However, not all the particles were levitated, but some particles were transported on the lower electrode. There were few particles above the upper electrode; thus, the Coulomb forces might be not very large. For V_L = +5 kV and V_U = 0 (Fig. 6b), as the electric field strength was larger, the particles experienced larger Coulomb forces. Most of the particles moved upward and some particles reached the mesh electrode or passed through it. Basically, the particles levitated from the positive electrode are charged positively, while the particles levitated from the negative electrode are charged negatively. Therefore, the particles between the upper and lower electrodes have positive and negative charges. For V_L = +8 kV and V_U = 0 (Fig. 6c), the applied voltage was much larger; thus, the particles could experience much larger Coulomb forces. As a result, particle velocities passing through the mesh electrode could be much higher. On the other hand, as shown in Fig. 6d, when the lower electrode was grounded, and an external voltage was applied to the upper electrode, i.e. V_L = 0 and V_U = −8 kV, the particles were more widely spread above the upper electrode. Most of the particles passed through the mesh electrode and were finally attracted to the upper electrode. When the particles were negatively charged on the upper electrode by induction charging, these particles could be re-levitated and experience upward Coulomb forces above the upper electrode.

Fig. 7 shows cumulative distribution curves of particle positions in the z-direction for different external voltages. These results were obtained by collecting the particles on a polypropylene plate with an adhesive material. The adhesive plate was temporarily placed in

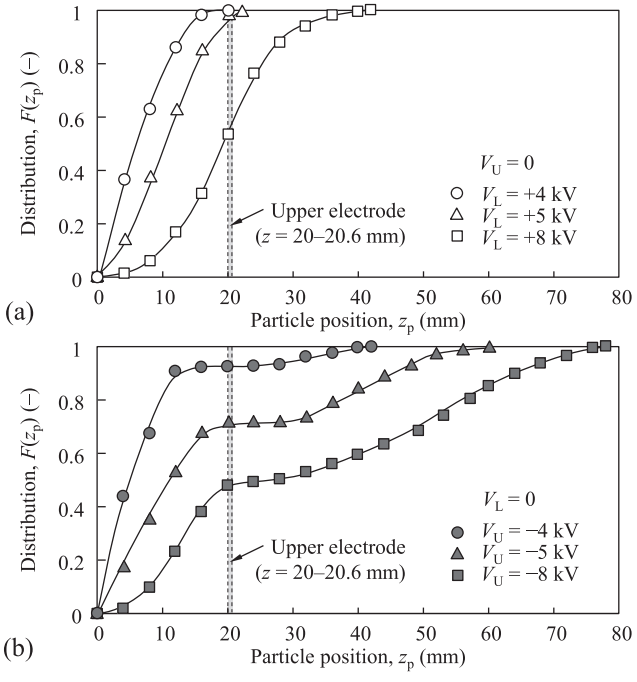

Fig. 7. Cumulative distributions of particle positions in the z-direction for different external voltages: (a) V_U = 0 and V_L > 0; and (b) V_L = 0 and V_U < 0.

the z-direction at a distance of 3 mm from the end edge of the electrodes. For V_U = 0 and V_L > 0 (Fig. 7a), the range of the particle position increased with an increase in the value of V_L. For $V_L \leq$ +5 kV, the particle positions were distributed between the electrodes,

i.e. in the range from 0 to 20 mm. For V_L = +8 kV, the maximum levitation height was over 40 mm. These distribution curves were monomodal. The range of the particle position for V_L = 0 and V_U < 0 (Fig. 7b) also increased with increasing absolute value $|V_U|$. This tendency is the same as that shown in Fig. 7a; however, the height range is obviously wider. Even for $|V_U|$ = 4 kV, the maximum levitation height was higher than the upper electrode. For $|V_U|$ = 8 kV, the maximum height was almost 80 mm. These distribution curves were found to be bimodal, i.e. the first distribution range was smaller than approximately 30 mm and the second one was larger than approximately 30 mm. The percentage of the particles located at the higher position increased with an increase in $|V_U|$. These results imply that there are two different phenomena in particle charge and levitation.

Fig. 8 illustrates the scenarios of the charging and the motion of particles expected in this system. External voltage is applied to one of the electrodes and the other electrode is grounded. The upper virtual boundary is assumed to be zero. For V_U = 0 and V_L > 0 (Fig. 8a), the electric field between the upper and lower electrodes is directed upward. Particles that are charged positively on the lower electrode experience upward Coulomb forces. The levitated particles can pass through the mesh electrode owing to particle inertia but the Coulomb forces above the upper electrode are smaller than the gravitational forces; hence, there are limits on the maximum heights of the particles. These particles are finally attracted to the upper electrode. After adhesion, their polarity can be changed by the induction charging. The negatively charged particles levitate from the upper electrode. However, the Coulomb forces above the upper electrode drastically decrease with increasing height; therefore, the particles cannot reach higher positions. For V_U = 0 and V_L < 0 (Fig. 8b), the electric field between the two electrodes is directed downward and the particles are charged negatively on the lower electrode. The polarities of the particles are opposite to those in Fig. 8a; however, the Coulomb forces acting on the particles are the same. As a result, the motions of the particles are the same as in Fig. 8a.

The particle motions in Fig. 8c are different from those in Fig. 8a. When V_U < 0, two electric fields are formed; one is directed upward between the two electrodes and the other is directed downward above the upper electrode. Once the particles adhere to the upper electrode, the polarity of the particles is changed. Since the Coulomb forces above the upper electrode are directed upward, the particles can reach higher positions. As a result, the polarity of the charged particles at the higher position is opposite to that of the particles levitated from the lower electrode. The polarities in Fig. 8d are completely opposite to those in Fig. 8c; however, the motions of the particles are the same as in Fig. 8c.

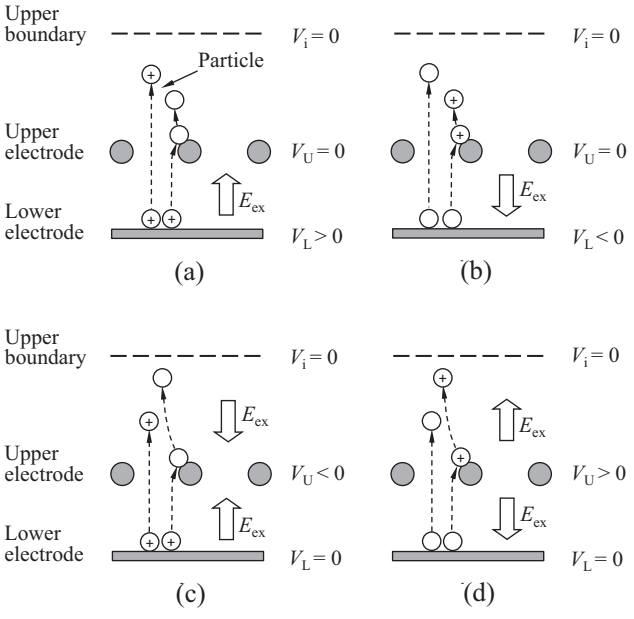

Fig. 8. Scenarios of the charging and the motion of particles expected in this system: (a) V_U = 0 and V_L > 0; (b) V_U = 0 and V_L < 0; (c) V_L = 0 and V_U < 0; (d) V_L = 0 and V_U > 0.

6.2. Particle charge

Fig. 9 shows the relationship between the specific charge of the particles (q_m) and the potential difference between the two electrodes ($\Delta V_{L-U} = V_L - V_U$). The experimental results were obtained under two different conditions; i.e., V_U = 0 (open symbols) and V_L = 0 (closed symbols). The q_m values were measured by collecting all the particles in the Faraday cup.

For V_U = 0, which corresponds to Fig. 8a and b, q_m has a positive correlation with ΔV_{L-U}. When the absolute value of the potential difference is small ($|\Delta V_{L-U}| < 4$ kV), the particles levitated from the lower electrode cannot reach the upper electrode (see Figs. 6a and 7a). The polarity of the particles is the same as that of the lower electrode. For $|\Delta V_{L-U}| \approx 4$ kV, some particles adhere to the upper electrode, and the polarity of the charged particles can be changed. As a result, the dependency of ΔV_{L-U} on q_m decreases somewhat. When $|\Delta V_{L-U}| > 4$ kV, particles can pass through the mesh electrode. The quantity of the particles charged on the lower electrode apparently increases; consequently, the dependency of ΔV_{L-U} on q_m increases again.

For V_L = 0, which corresponds to Fig. 8c and d, the experimental data at $|\Delta V_{L-U}| > 4$ kV are different from those for V_U = 0, i.e., q_m has a negative correlation with ΔV_{L-U}. This is because the polarity of the charged particles at the higher position is opposite to that of the particles levitated from the lower electrode, and also because the percentage of the particles at the higher positions increases with increasing $|\Delta V_{L-U}|$.

6.3. Motion of charged particles

Fig. 10 shows a series of motions of a particle in an electric field observed by the high-speed microscope camera and the specific charge of the particle estimated from the particle motion analysis mentioned in Section 4. The upper figure indicates the particle position in the *z*-direction as a function of elapsed time. The experimental results (solid lines) agree well with the results calculated

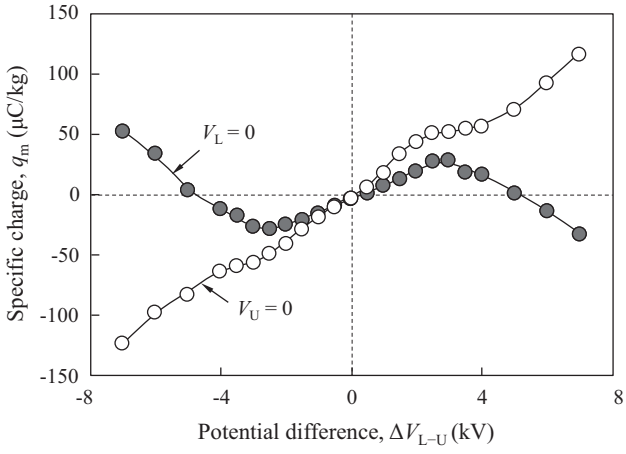

Fig. 9. Relationship between the specific charge of the particles and the potential difference between the two electrodes ($\Delta V_{L-U} = V_L - V_U$).

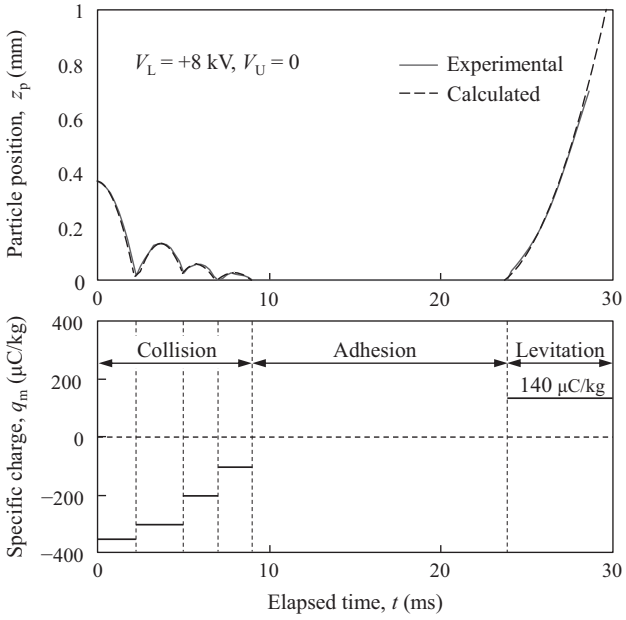

Fig. 10. Motion of a particle observed in an electric field and the specific charge of the particle estimated from the particle motion (V_L = +8 kV and V_U = 0).

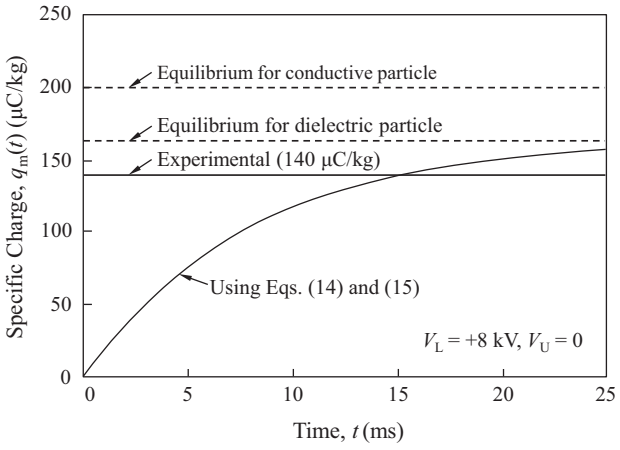

Fig. 11. Analysis of induction charging of primary particle (V_L = +8 kV and V_U = 0).

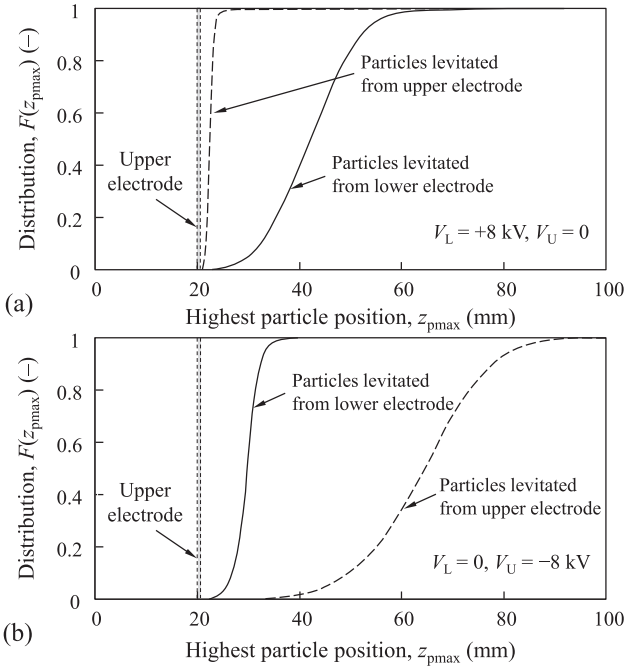

Fig. 12. Calculated distributions of highest particle positions in the z-direction for different external voltages: (a) V_L = +8 kV, V_U = 0; and (b) V_L = 0, V_U = −8 kV.

based on the equation of motion (broken lines), where the fitting parameter is the particle charge q_p. The lower figure indicates the variation of the specific charge q_m that was obtained from the q_p values. From these results, the particle motion can be classified into three categories, i.e., collision, adhesion, and levitation. In the collision process, the charged particle was attracted to the lower electrode by the Coulomb force, and repeatedly collided with decreasing rebound height. The negative charge on the particle decreased with the number of collisions because the particle acquired some positive charge during each collision with the positive electrode. After losing its kinetic energy, the particle adhered to the electrode. As the particle acquired a larger positive charge by the induction charging for a period of 15 ms, the polarity of the particle was changed from negative to positive. When the Coulomb force directed upward became sufficiently large, the particle was levitated. Although the specific transferred charge Δq_m during a collision were less than 100 μC/kg, Δq_m during the adhesion was more than 200 μC/kg. It is worth noting that the contact time is important for the charge transfer. After the levitation, the specific charge was 140 μC/kg., which is 70% of the equilibrium charge caused by the induction charging for conductive materials [7]. If the forces directed downward, such as adhesion and gravity, were much larger, the specific charge would be larger than 140 μC/kg, which would result in a longer contact time.

Fig. 11 shows the analysis of the induction charging of the levitated particle shown in Fig. 10. The specific charge of a dielectric particle (solid curve) was calculated using Eq. (14) with τ = 8 ms, which was obtained using Eq. (15), i.e., 0.1 GΩ m × 8.85 × 10^{-12} F/m × 9. The calculated value reached the experimental value (140 μC/kg) at 15 ms. This contact time agreed with the value for the levitation shown in Fig. 10. For reference, the equilibrium charges of the dielectric and conductive particles are also shown in the same figure.

Fig. 12 shows the calculated distributions of highest particle positions in the z-direction, which depend on the particle charge and the electric field. The particles can be levitated from the lower electrode and the upper electrode. In the former case, particles were presumed to be levitated from the point of x = 0 mm and y = 0 mm that was the center of the wire mesh opening and z = 0 mm that was the surface of the lower electrode; thus, the particles could pass through the mesh electrode. In the latter case, the initial point of the particles was presumed to be x = 2.12, y = 0 and z = 20.6 mm that was the top surface of the mesh wire. For the two cases, the electric fields calculated in Fig. 3a and b were used to estimate the Coulomb forces. The initial particle charge was presumed to be positive on the lower electrode and negative on the upper electrode considering the induction charging. Furthermore, the initial charges were assumed to have a normal distribution with an average value of ±130 μC/kg and a standard deviation of 33.2 μC/kg, which were based on preliminary experimental results.

For V_L = +8 kV and V_U = 0 (Fig. 12a), the highest positions of the particles levitated from the lower electrode (solid line) were in a range from 20 to 60 mm, showing that all the particles can pass through the mesh electrode and reach higher positions. However, the particles levitated from the upper electrode (broken line) were held close to the upper electrode. This difference in the particle

height can be explained as follows; the particles move upward below the upper electrode owing to their Coulomb forces and have large velocities or large inertial forces; consequently, the particles can reach higher positions even though the gravitational forces are dominant. The particles levitated from the upper electrode also move upward; however, these particles do not have large inertial forces, and the Coulomb forces immediately become zero; thus, the particle height is rather low.

For $V_L = 0$ and $V_U = -8$ kV (Fig. 12b), the distribution range of the particles levitated from the upper electrode shifts to very high positions. This is because a downward electric field is formed above the upper electrode (see broken lines in Fig. 3), and the particles levitated from the upper electrode have negative charges. Therefore, the particles continue to experience upward Coulomb forces. On the other hand, the range for the particles levitated from the lower electrode was from 20 to 40 mm (solid line). These particles have positive charges, and experience downward Coulomb forces above the electrode. As a result, the particle position was lower than the solid line in Fig. 12a.

7. Summary and conclusions

Electrification and levitation of particles in a continuous particle feed and dispersion system with vibration and external electric fields were studied both theoretically and experimentally. In this system, a mesh electrode and a vibrating plate electrode were used for the upper and lower electrodes, respectively. The specific charge of the particles was measured by collecting all the particles in the Faraday cup, and the particle behavior was observed microscopically. Furthermore, the particle charges were determined from experimentally obtained particle trajectories and numerically calculated electric fields. The results obtained can be summarized as follows:

(1) The particles are levitated from the electrode and dispersed by applying an external voltage. When the voltage is applied to the upper electrode, the particles are more widely spread above the upper electrode than when the voltage is applied to the lower electrode. The spread area of the particles also increases with an increase in the absolute value of the applied voltage.
(2) The specific charge strongly depends on the potential difference between the two electrodes. When the voltage is applied to the upper electrode, the variation of the specific charge is more complicated depending on the motion of the particles.
(3) The motion of the particles around the electrode is classified into three categories, i.e., collision, adhesion, and levitation. In the collision process, the charged particles are attracted to the opposite electrode by the Coulomb forces and collide with the electrode. When the impact of the particle collision is large, the particles rebound and collide repeatedly. The charge on the particles decreases with an increase in the number of collisions. After the particles adhere to the electrode and acquire a large quantity of charge by induction, they are levitated again. The charge transferred during adhesion is larger than that transferred during a collision, i.e., the charge transfer for dielectric or semiconductive materials depends on the contact time.
(4) The height of levitation of a charged particle can be estimated by calculating the particle trajectory in the electric field.

Acknowledgement

This research was supported by JSPS Grant Number JP17H03442.

References

[1] S. Matsusaka, W. Theerachaisupakij, H. Yoshida, H. Masuda, Deposition layers formed by a turbulent aerosol flow of micron and sub-micron particles, Powder Technol. 118 (2001) 130–135.
[2] H. Masuda, K. Gotoh, H. Fukada, Y. Banba, The removal of particles from flat surfaces using a high-speed air jet, Adv. Powder Technol. 5 (1994) 205–217.
[3] K. Gotoh, K. Mizutani, Y. Tsubota, J. Oshitani, M. Yoshida, K. Inenaga, Enhancement of particle removal performance of high-speed air jet by setting obstacle in jet flow, Particul. Sci. Technol. 33 (2015) 567–571.
[4] I.M. Zainuddin, M. Yasuda, T. Horio, S. Matsusaka, Experimental study on powder flowability using vibration shear tube method, Part. Part. Syst. Char. 29 (2012) 8–15.
[5] M. Adachi, K. Hamazawa, Y. Mimuro, H. Kawamoto, Vibration transport system for lunar and Martian regolith using dielectric elastomer actuator, J. Electrostat. 89 (2017) 88–98.
[6] H. Masuda, Dry dispersion of fine particles in gaseous phase, Adv. Powder Technol. 20 (2009) 113–122.
[7] A.Y.H. Cho, Contact Charging of micron-sized particles in intense electric fields, J. Appl. Phys. 35 (1964) 2561–2564.
[8] Y. Ohkubo, Y. Takahashi, Lifting criteria of an induction-charged spherical particle in a field with horizontally set parallel plate electrodes, Kagaku Kogaku Ronbun. 22 (1996) 113–119.
[9] Y. Ohkubo, Y. Takahashi, Experimental investigation on lifting criteria of an induction-charged spherical particle in a field with horizontally set parallel plate electrodes, Kagaku Kogaku Ronbun. 22 (1996) 603–609.
[10] Y. Wu, G.S.P. Castle, I.I. Inculet, S. Petigny, G.S. Swei, Induction charge on freely levitating particles, Powder Technol. 135 (2003) 59–64.
[11] B.F. Nader, G.S.P. Castle, K. Adamiak, Effect of surface conduction on the dynamics of induction charging of particles, J. Electrostat. 67 (2009) 394–399.
[12] S. Matsusaka, H. Maruyama, T. Matsuyama, M. Ghadiri, Triboelectric charging of powders: a review, Chem. Eng. Sci. 65 (2010) 5781–5807.
[13] S. Matsusaka, Control of particle tribocharging, Kona Powder Part. J. 29 (2011) 27–38.
[14] T. Tada, T. Yamamoto, Y. Baba, M. Takeuchi, Ion charging and electron charging to an insulating toner, J. Soc. Powder Technol. Japan 41 (2004) 636–644.
[15] S. Masuda, K. Fujibayashi, K. Ishida, H. Inaba, Confinement and transportation of charged aerosol clouds via electric curtain, Electr. Eng. Jpn. 92 (1972) 43–52.
[16] S. Matsusaka, K. Yoshitani, H. Tago, T. Nii, H. Masuda, T. Iwamatsu, Sampling of charged fine particles by motion control under AC Field, J. Soc. Powder Technol. Japan 45 (2008) 387–394.
[17] H. Kawamoto, Some techniques on electrostatic separation of particle size utilizing electrostatic traveling-wave field, J. Electrost. 66 (2008) 220–228.
[18] R.K. Dwari, S.K. Mohanta, B. Rout, R.K. Soni, P.S.R. Reddy, B.K. Mishra, Studies on the effect of electrode plate position and feed temperature on the tribo-electrostatic separation of high ash Indian coking coal, Adv. Powder Technol. 26 (2015) 31–41.
[19] M.K. Mazumder, R. Sharma, A.S. Biris, J. Zhang, C. Calle, M. Zahn, Self-cleaning transparent dust shields for protecting solar panels and other devices, Particul. Sci. Technol. 25 (2007) 5–20.
[20] H. Kawamoto, M. Uchiyama, B.L. Cooper, D.S. McKay, Mitigation of lunar dust on solar panels and optical elements utilizing electrostatic traveling-wave, J. Electrost. 69 (2011) 370–379.
[21] M. Blajan, Y. Mizuno, A. Ito, K. Shimizu, Microplasma actuator for EHD induced flow, IEEE T. Ind. Appl. Soc. 59 (2017) 2409–2415.
[22] M. Adachi, H. Maezono, H. Kawamoto, Sampling of regolith on asteroids using electrostatic force, J. Aerospace Eng. 29 (2016) 04015081.
[23] H. Kawamoto, A. Shigeta, M. Adachi, Utilizing electrostatic force and mechanical vibration to obtain regolith sample from the moon and mars, J. Aerospace Eng. 29 (2016) 04015031.
[24] S. Matsusaka, J. Iyota, M. Mizutani, M. Yasuda, Characterization and control of particles triboelectrically charged by vibration and external electric field, J. Soc. Powder Technol. Japan 50 (2013) 632–639.
[25] M. Mizutani, M. Yasuda, S. Matsusaka, Advanced characterization of particles triboelectrically charged by a two-stage system with vibrations and external electric fields, Adv. Powder Technol. 26 (2015) 454–461.
[26] M. Shoyama, S. Matsusaka, Electric charging of dielectric particle layers and levitation of particles in a strong electric field, Kagaku Kogaku Ronbun. 43 (2017) 319–326.
[27] L. Schiller, A. Naumann, A drag coefficient correlation, Z. Ver. Dtsch. Ing. 77 (1935) 318–320.
[28] M. Hywel, N.G. Green, Dielectrophoretic manipulation of rod-shaped viral particles, J. Electrost. 42 (1997) 279–293.